Thermal Properties and Crystallization Behaviors of Polylactide and Its Enantiomeric Blends

Pakorn Opaprakasit,[*1] *Mantana Opaprakasit*[2]

Summary: Thermal properties and crystallization behaviors of polylactide and its enantiomeric blends are investigated. DSC results demonstrate that only homopolymer crystallite is observed in PDLA and PLLA single polymers. A relatively stronger crystal structure, stereocomplex, can be achieved by mixing the two PLAs in a 1:1 ratio. For non-equimolar blends, both types of crystallites are formed at lower temperature than that of the single polymer counterparts. The degree of reduction in crystallization temperature is dependent on the degree of deviation of blend content from the equimolar value and the mobility of the polymer chain. The composition of the two crystallite domains is also dependent on the blend content, where the stereocomplex content is maximized in a 1:1 blend, and decreases upon varying the mixing ratio from equimolar value. Infrared spectroscopy is employed to follow the crystallization mechanisms of the non-equimolar blend. Results indicate a domination of stereocomplex formation band characteristics, despite evidences suggesting an existent of homopolymer crystallite formation, probably due to the involvement of C–H··O=C hydrogen bonding, which leads to larger change in dipole moment responsible for infrared transitions.

Keywords: C–H··O=C hydrogen; crystallization; polylactide; stereocomplex; thermal properties

Introduction

Polylactide (PLA) is a well known biopolymer. This thermoplastic is of interest in various applications, for example, medical, packaging, and agricultural applications; because of its biocompatibility, degradability, and mechanical properties that are comparable to those of commodity plastics.[1–5] Most importantly, the monomer constituent of this polymer can be derived from renewable resources such as corn, cassava, and sugar cane.

As its repeat unit consists of a carbon chiral center, PLA is presented in two enantiomeric isomers: poly(D-lactide) PDLA, and poly(L-lactide), PLLA. The two isomers adopt an opposite helical conformation in solid state. It has been reported that a racemic crystal structure or stereocomplex can be obtained by mixing the two enantiomeric PLAs.[6] This stereocomplex, in turn, showed a higher melting temperature (~50 °C) than that of its single component counterpart.[7] Accordingly, this stereocomplex has received some attention as potential high performance biodegradable materials. Crystallization mechanisms of stereocomplex in comparison with its single component counterparts have been extensively studied to obtain an insight into the differences in their crystal structures and crystallization mechanisms.[8,9] Recently, reports on the involvement of unconventional C–H··O=C hydrogen bonding in the crystal structure

[1] Department of Common and Graduate Studies, Sirindhorn International Institute of Technology (SIIT), Thammasat University, Pathumthani 12121 Thailand
Fax +662-986-9009 Ext. 1806;
E-mail: pakorno@gmail.com
[2] Department of Materials Science, Faculty of Science, Chulalongkorn University, Bangkok, 10330 Thailand

of stereocomplex have gained popularity.[10,11]

In our recent study,[12] we observed weak vibrational modes in the ~3,500 cm^{-1} region of the PLA infrared spectra, and assigned the bands to overtone combination modes of carbonyl stretching. The bands were used to follow the correlation of changes between C=O and C–H groups during crystallization by employing 2D-FTIR correlation spectroscopy. The results showed that C–H··O=C hydrogen bonding interaction accompanied the formation of stereocomplex, while interaction associated with crystal formation of PLA single polymer was induced dipole interaction.

In this communication, thermal properties and the mechanisms of crystallization and melting process of PLA single polymers and their blends are examined by employing DSC and FTIR experiments.

Experimental Part

Relatively low molecular weight PLLA (low-PLLA, $M_v = 3.2 \times 10^3$) was purchased from Birmingham Polymers. High-MW PLLA (high-PLLA, $M_v = 1.4 \times 10^4$) and PDLA ($M_v = 8.7 \times 10^4$) was supplied by Cargill Dow Polymers and PURAC Biochem, respectively. Blends of PLLA and PDLA were prepared by separately dissolving each component in dichloromethane. The two solutions were then mixed in desired compositions and stirred vigorously for 24 hours. Two series of blends were prepared. Low-MW blends consist of low-PLLA and PDLA and are referred to as LB series e.g. LB64 consists of 60:40 PDLA/low-PLLA. Similarly, the high-MW blend series is referred to as HB series (e.g. HB55).

Thermal properties and in-process crystallization and melting of the samples were determined using a Perkin Elmer DSC7. Samples were scanned from 30 to 250 °C at a heating rate of 10 °C/min. Crystallization mechanisms of PLA and its blends were investigated by FTIR spectroscopy. A film sample was prepared by casting the solutions on a glass slide. The samples were then melted at 240 °C in a Mettler (model FP-82) hot-stage and quenched in ice water to completely erase its thermal history. FTIR spectra were recorded on a Nicolet model 6700 spectrophotometer at a resolution of 2 cm^{-1}. A ''HARRICKS'' temperature controller was used in the measurements of infrared spectra as a function temperature and crystallization time. Cold-crystallization was carried out by heating the amorphous samples to, and keeping them, at 80 °C. Melt-crystallization was performed at 120 °C after by heating the sample to 240 °C for 5 minutes to erase its thermal history. FTIR spectra were recorded as a function of time at 30 second intervals.

Results and Discussion

Thermal properties of amorphous PLAs and theirs blends were studied by employing DSC experiments. Glass transition temperature (T_g) of PDLA, high-PLLA, and low-PLLA were observed at 58, 56, and 40 °C, respectively. Single T_g was observed for all corresponding blends, whose values are shown as a function of PDLA content in Figure 1. The results obtained from both high-MW blend (HB) and low-MW (LB) blend series agree with the trend predicted from the Fox equation. This indicates miscibility between these enantiomeric PLAs at a length scale of ~10 nm, the approximately experimental probe size of DSC.

In-process crystallization and melting behaviors of PLA single polymers and blends were examined. Thermograms of the samples recorded from the glassy state to above T_m are shown in Figure 2 and Figure 3. Crystallization exotherms (T_c) and melting endotherms (T_m) of high-PLLA, and PDLA are significantly comparable ($T_c \sim 105$ °C, $T_m \sim 175$ °C), reflecting the independence of T_c and T_m on structural configurations. In contrast, the corresponding exotherm and endoterm of

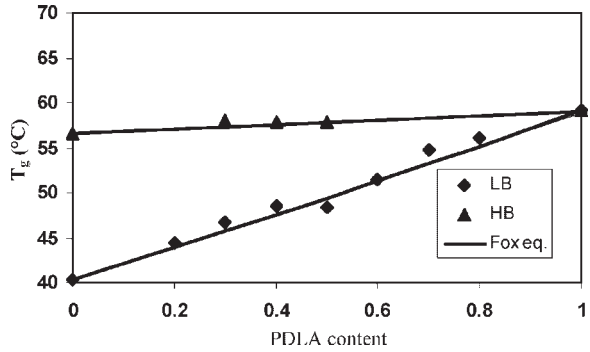

Figure 1.
Experimental T_g's of PDLA/low-PLLA (◆) and PDLA/high-PLLA (▲) as a function of PDLA content, and the predicted T_g from the Fox-Flory equation (solid lines).

the low-PLLA was observed at 80 and 160 °C, respectively. This indicates that the shorter-chain PLLA has more flexibility to organize and form crystal structure at lower temperature. The low MW is also responsible for the reduction of the melting point. The observed T_m of stereocomplex from the blends is, however, increased to 215 °C, indicating a relatively stronger crystal structure.

Crystallization of PDLA/high-PLLA blends depends strongly on blend composition, where T_c was observed at temperatures lower than that of the single polymer counterparts. The lowest T_c of the blends was observed in the equimolar blend (HB55) at 97 °C, much lower than those obtained from its single polymer constituents (See Figure 2). When the blend composition is deviated from a 1:1 ratio, crystallization takes place at slightly higher temperature, i.e., 98 and 99 °C for HB64 and HB73, respectively. This is because a formation of stereocomplex is favored to homopolymer crystallite formation, hence taking place at lower temperature. In HB55 equimolar blend, only stereocomplex is formed, reflecting by a single T_m located at 215 °C. This results in crystal formation occurring at the lowest temperature. When

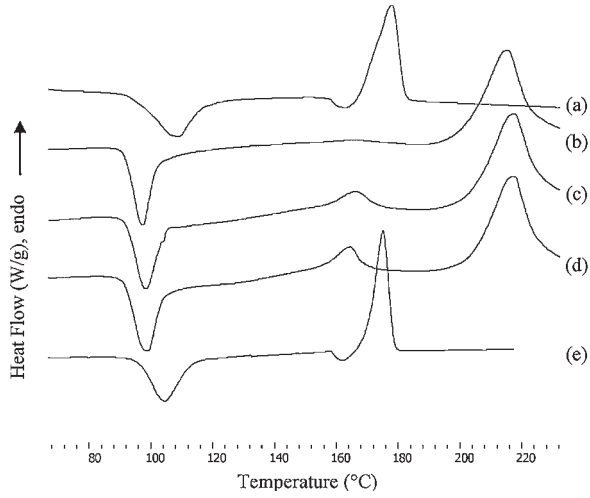

Figure 2.
DSC thermograms of neat PDLA(a), high-PLLA(e), and PDLA/high-PLLA blends: HB55(b), HB64(c), HB73(d).

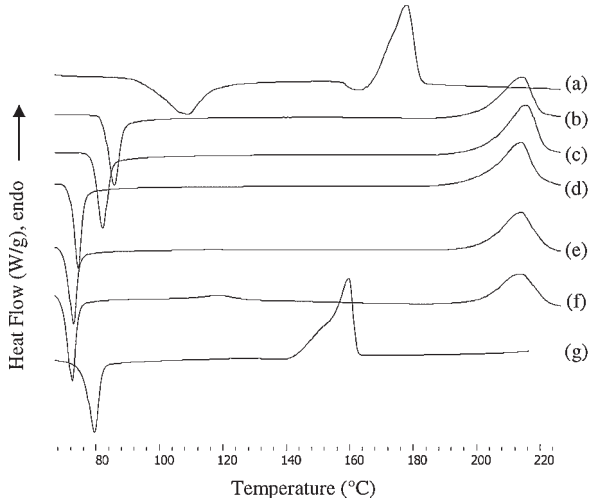

Figure 3.
DSC thermograms of neat PDLA(a), low-PLLA(g), and PDLA/low-PLLA blends: LB28(b), LB37(c), LB55(d), LB73(e), and LB82(f).

excess amount of high-PLLA is presented in the blends, i.e. HB64 or HB73, a mixture of stereocomplex and single crystallite was observed, as indicated by 2 T_m's at 215 and 165 °C, respectively. This results in a slight increase in the observed T_c's, compared to that of HB55.

DSC thermograms of low-MW blends series are shown in Figure 3. Unlike the previous blend series, the results indicate that T_c is dependent on two factors; the blend composition and the content of the low-MW constituent. T_c of the PDLA-rich blends decreases, upon increasing of low-PLLA content, from 86, 82, and 74 °C for LB28, LB37, and LB55, respectively. However, further increasing of the low-PLLA content in the PLLA-rich blends enables the chain to crystallize at lower temperature. (T_c of LB73 and LB82 were observed at 73 and 72 °C, respectively.) This is probably because the crystal formation of these blends is affected by the mobility provided from the low-PLLA, which enables the co-crystallization of the two enantiomeric chains to form stereocomplex. Surprisingly, the thermograms of the blends show single T_m of the stereocomplex at 215 °C for the blend that contains low-PLLA of up to 70%, where the T_m of homopolymer crystallite appears when content of low-PLLA reaches 80% (LB82). This can be explained in term of restriction of PLLA homopolymer crystallite formation from stereocomplex domain. The more flexible shorter low-PLLA chains promote the stereocomplex formation. The crystal structure, in turn, lowers the flexibility of the excess PLLA fraction to organize, hence remain in amorphous phase until significant amount of excess PLLA is reached (i.e. LB82).

An insight into the influence of blend composition on fractions of the two crystallites was further investigated when the polymers chains are allowed to crystallize at a constant temperature. The samples were first isothermally crystallized at 70 °C for 30 minutes, and their DSC thermograms were then recorded. The results obtained from low-MW blend series indicate two T_m's derived from homopolymer crystallite and stereocomplex for all samples. The crystal composition was obtained from the ratios of ΔH_m of the two endotherms, as shown in Figure 4. The maximum stereocomplex content is obtained in the equimolar blend. A reduction in the racemic crystallite content is observed for blends with PDLA content >0.5 or <0.5, and vice versa for

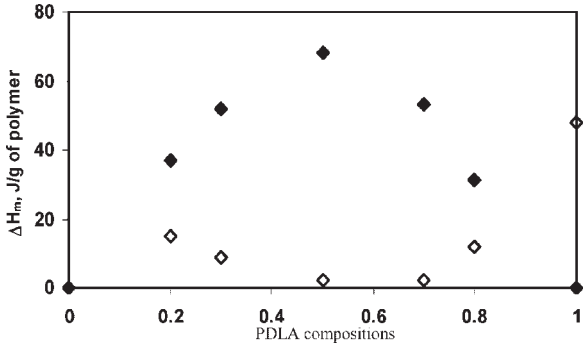

Figure 4.
Crystal domain composition represented by ΔH_m of PDLA/low-PLLA blends after crystallization at 70 °C, where closed and open symbols represent the stereocomplex and the homopolymer crystallite, respectively.

homopolymer crystallite, which is similar to that reported previously for blends of similar molecular weight[13,14].

In our recent study,[12] we found that weak vibrational modes were observed in the ~3,500 cm^{-1} region of the PLA infrared spectra. These were assigned to overtone combination modes of carbonyl stretching. At least two vibrational modes were observed in the different spectra as a function of crystallization time of PLA and its 1:1 blend. The patterns of intensity change of the two systems are different; in PLLA or PDLA single polymers, a 3510 cm^{-1} mode increases in intensity, while the lower frequency mode at 3482 cm^{-1} decreases. On the other hand, the intensity of the higher frequency mode at 3510 cm^{-1} decreases, while the 3480 cm^{-1} band increases for HB55 blend (stereocomplex formation). Subsequently, the bands were used to follow the correlation of changes between C=O and C–H groups during crystallization by employing 2D-FTIR correlation spectroscopy. The results showed that the two groups changed simultaneously in the stereocomplex, indicating an involvement of C–H··O=C hydrogen bonding. In contrast, results observed in PDLA single polymer spectra showed that C=O group change preceding that of C–H group, reflecting an involvement of induced dipole interaction.

The infrared band of C–H stretching mode also indicates different interactions associated with the formation of homopolymer crystallite and stereocomplex. In single polymer, the frequency of the asymmetric C–H_3 stretching mode at 2995 cm^{-1} shifts to higher frequency, indicating lateral interchain interaction, while those of the C_α–H mode at 2880 cm^{-1} remain unchanged[15]. In the formation of stereocomplex, however, the C–H_3 stretching mode now red-shifts to lower frequency at 2992 cm^{-1}. This is due to the involvement of C–H··O–C hydrogen bonding. The explanation for the red-shift is because of the attractive interaction between the C–H and C=O that leads to the elongation of the C–H bonds.[16]

To obtain insight into crystallization mechanism of blends that consists of unequal amount of enantiomeric constitutes, infrared spectra of HB73 blend were examined. Figure 5 shows the difference spectra as a function of cold-crystallization time in the C=O overtone, C–H stretching, and C–C coupling C–H modes. The results indicates a domination of intensity change patterns similar to that found in the equimolar (HB55) blend, i.e. the intensity reduction of 3480 cm^{-1} mode, the increase of 3510 cm^{-1} band, the red-shift of CH_3 stretching modes, and the increase in intensity of the crystal characteristic at 908 cm^{-1}. These results suggest a formation of the stereocomplex. Surprisingly, the band characteristic of homopolymer crystallite formation cannot be observed,

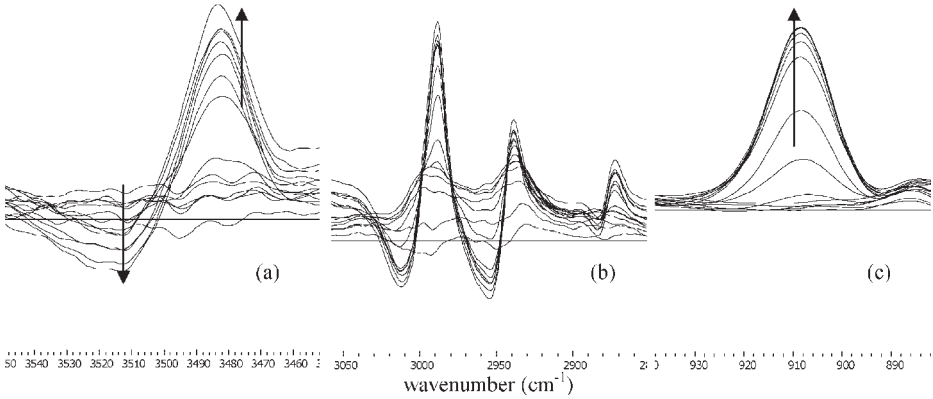

Figure 5.
Difference infrared spectra as a function of cold-crystallization time; in the C=O overtone (a), C–H stretching (b), and C–C backbone coupling C–H modes (c).

despite clear evidences from DSC indicating that the existent of particular formation. DSC thermogram of the same sample shows two T_m's upon isothermal crystallization at the same temperature, with ΔH_m ratio of 52/10.

The different spectra obtained during melting process after cold crystallization, as shown in Figure 6, also indicate two melting mechanisms, associated with homopolymer crystallite and stereocomplex. As the temperature reaches 160 °C, a reverse intensity-change pattern to the formation of homopolymer crystallite was observed. The opposite change pattern (a reverse trend to that observed in stereocomplex formation), however, appears when the temperature was raised above the melting point of stereocomplex (>240 °C). This, in good agreement with DSC results, indicates that two difference domains of crystals were formed during cold crystallization. The significant domination of stereocomplex band characteristics in the infrared spectra is probably because the structure is more thermodynamically stable and asso-

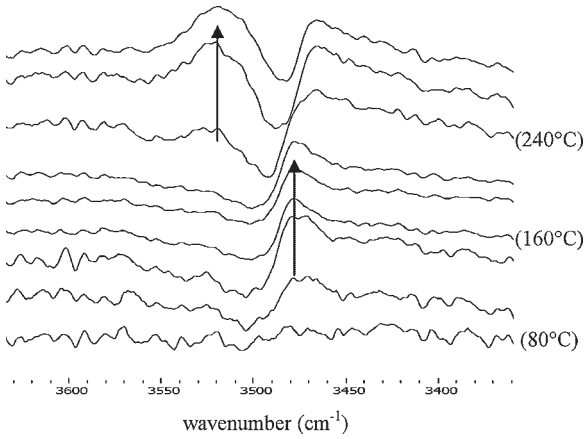

Figure 6.
Difference infrared spectra recorded during melting process of HB73 after isothermal crystallization at 70 °C for 30 minutes.

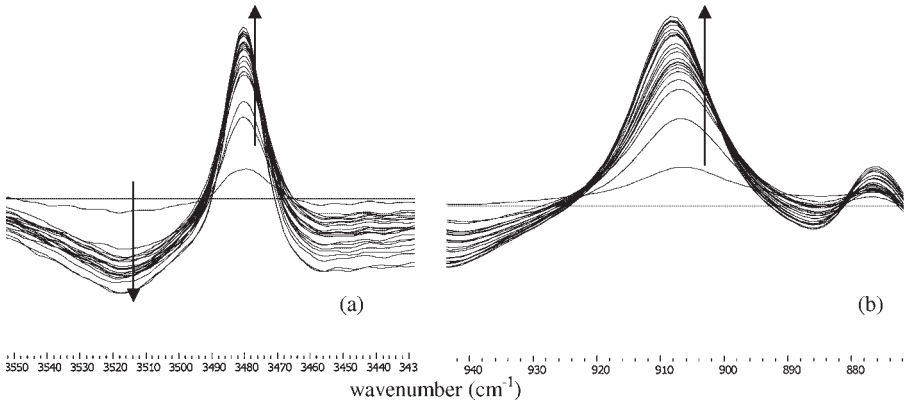

Figure 7.
Difference infrared spectra as a function of melt-crystallization time; in the C=O overtone (a) and C–C backbone coupling C–H modes (b).

ciated with stronger interactions, compared to homopolymer crystallite, resulting in larger dipole transitions that are responsible for infrared absorption.

The dynamic spectra obtained during melt-crystallization of the HB73 blend at 120 °C are shown in Figure 7. The patterns of change are similar to those observed in the cold-crystallization process, i.e. largely dominated by stereocomplex characteristics. Kinetic of the two crystallization process are compared by employing the intensity of C–C coupling C–H vibrational mode at 908 cm^{-1}, as shown in Figure 8. The results show that longer induction time is required in the cold crystallization, as the mobility of chains is limited compared to that in the melt crystallization. However, the growing rate of the crystal formation is comparable, reflecting the strong interaction accompanied the formation process.

Conclusions

Results from DSC experiments on PLA enantiomeric blends reveal that PDLA and PLLA are miscible for all composition. Crystallization of the blends is taking place at lower temperature, compared to that of the single component counterparts, and the degree of reduction is dependent on the

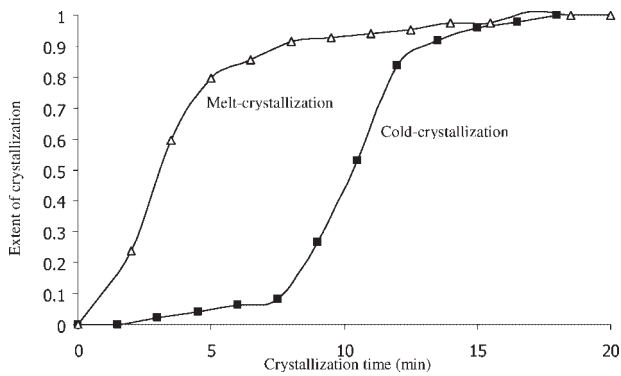

Figure 8.
Extent of crystal formation calculated from band intensity of the 904 cm^{-1} mode: cold-crystallization at 70 °C, and melt-crystallization at 120 °C.

blend composition and chain mobility. A formation of stereocomplex is observed in equimolar blend. When the blend composition is deviated from a 1:1 ratio, two domains of crystal structures are developed. The stereocomplex content is maximized when 1:1 PDLA/PLLA is blended. The racemic structure content decreases upon varying the composition from the equimolar value. Crystallization mechanism of the non-equimolar blend is also examined by employing FTIR spectroscopy. The band characteristics of stereocomplex formation dominate the change in both cold- and melt-crystallization processes, despite a combination of homopolymer crystallite and stereocomplex formation is taking place.

Acknowledgements: Financial supports of this work are provided by the Thailand Research Fund (TRF) and the Commission of Higher Education of Thailand (CHE), under grant no. DE-FG02-86ER13537. The authors are grateful for technical support and discussion from Prof. Pramaun Tangboriboonrat, Mahidol University. We also thank Prof. James Runt, Penn State University, for the use of DSC instrument and helpful discussion.

[1] J. W. Leenslag, A. J. Pennings, R. R. M. Bos, F. R. Rozema, G. Boering, *Biomaterials* **1987**, *8*, 311.
[2] A. Prokop, H. J. Helling, U. Hahn, C. Udomkaewkaujana, K. E. Rehm, *Clinical Orthopaedics and Related Research* **2005**, 226.
[3] Y. Kikkawa, H. Abe, T. Iwata, Y. Inoue, Y. Doi, *Biomacromolecules* **2002**, *3*, 350.
[4] H. Tsuji, S. Miyauchi, *Polymer Degradation and Stability* **2001**, *71*, 415.
[5] J. Y. Lim, S. H. Kim, S. Lim, Y. H. Kim, *Macromolecular Materials and Engineering* **2003**, *288*, 50.
[6] H. Tsuji, Y. Ikada, *Polymer* **1999**, *40*, 6699.
[7] Y. Ikada, K. Jamshidi, H. Tsuji, S. H. Hyon, *Macromolecules* **1987**, *20*, 904.
[8] E. Meaurio, E. Zuza, N. Lopez-Rodriguez, J. R. J. Sarasua, *Journal of Physical Chemistry B* **2006**, *110*, 5790.
[9] M. Kanchanasopa, *Ph.D. Dissertation*, The Pennsylvania State University, **2004**.
[10] Y. Hu, J. M. Zhang, H. Sato, Y. Futami, I. Noda, Y. Ozaki, *Macromolecules* **2006**, *39*, 3841.
[11] J. M. Zhang, H. Tsuji, I. Noda, Y. Ozaki, *Macromolecules* **2004**, *37*, 6433.
[12] P. Opaprakasit, M. Opaprakasit, P. Tangboriboonrat, *Applied Spectroscopy* **2007**, *61*, 1352.
[13] H. Tsuji, Y. Ikada, *Macromolecules* **1993**, *26*, 6918.
[14] S. Brochu, R. E. Prud'homme, I. Barakat, R. Jerome, *Macromolecules* **1995**, *28*, 5230.
[15] J. R. Sarasua, N. L. Rodriguez, A. L. Arraiza, E. Meaurio, *Macromolecules* **2005**, *38*, 8362.
[16] J. Joseph, E. D. Jemmis, *Journal of the American Chemical Society* **2007**, *129*, 4620.

